https://doi.org/10.5194/tc-2022-180
Preprint. Discussion started: 27 October 2022
© Author(s) 2022. CC BY 4.0 License.

The Cryosphere Discussions

Brief communication: The Impact of Interannual Melt Supply Variability on Greenland Ice Sheet Moulin Inputs

Tim Hill[1, *] and Christine F. Dow[1, 2]

[1]Department of Applied Mathematics, University of Waterloo, Waterloo, Canada
[2]Department of Geography and Environmental Management, University of Waterloo, Waterloo, Canada
[*]Current address: Department of Earth Sciences, Simon Fraser University, Burnaby, Canada

Correspondence: Tim Hill (tim_hill_2@sfu.ca)

Abstract. The supraglacial drainage system of the Greenland Ice Sheet, in combination with surface melt rate, controls the rate of water flow into moulins, driving subglacial water pressure. We apply a physically-based surface meltwater flow model to a $\sim 20 \times 27$ km^2 catchment on the southwestern Greenland Ice Sheet in high and low melt years to examine the impact of surface melt rate and variability on moulin inputs. The model outputs predict important differences in moulin inputs between high and low melt years. These dynamic model outputs will be important in driving future process-scale subglacial hydrology models.

1 Introduction

Mass loss from the Greenland Ice Sheet represents a major and accelerating contributor to global sea level rise (The IMBIE Team, 2020; Goelzer et al., 2020). Contemporary mass loss is nearly evenly partitioned between surface runoff and the discharge of grounded ice to the ocean (Mouginot et al., 2019; The IMBIE Team, 2020). While surface runoff is driven by atmospheric warming (van den Broeke et al., 2017), ice discharge is controlled by both warming of the atmosphere and ocean (e.g. Moon et al., 2012). One key process driving ice discharge and creating uncertainty in predictions is the dynamic relationship between surface melt and ice velocity.

This relationship between melt and ice flow is more subtle than suggested by early hypotheses of unmitigated surface melt-induced acceleration (e.g. Zwally et al., 2002). Higher surface melt rates and increased meltwater supply through moulins can improve the efficiency of the subglacial drainage system, allowing larger volumes of meltwater to be evacuated at lower pressure, in some cases leading to reduced summer-averaged ice flow in years with more surface melt (Sundal et al., 2011). Furthermore, some surface velocity measurements show that years with higher-than-average melt volumes are followed by lower-than-average winter velocities (Bartholomew et al., 2012; Sole et al., 2013).

The trade-off between surface melt and subglacial drainage suggests that melt supply variability on diurnal and seasonal timescales is more important than melt volume alone in driving summer velocities, especially in years with high melt where an efficient drainage system forms (Schoof, 2010; Bartholomew et al., 2012). Short-lived periods of high moulin discharge, including those caused by extreme surface melt events or rapid supraglacial lake drainage, to an efficient subglacial system can

https://doi.org/10.5194/tc-2022-180
Preprint. Discussion started: 27 October 2022
© Author(s) 2022. CC BY 4.0 License.


induce transient periods of high subglacial water pressure and ice flow. Between these melt pulses, ice flow relaxes towards its steady rate (Bartholomew et al., 2012).

Since the supraglacial drainage system delays and reduces the diurnal amplitude of melt inputs to moulins (Muthyala et al., 2022), it has the potential to significantly affect the relationship between surface melt and ice velocity. This "damp and delay" behaviour has been captured by supraglacial water flow models based on explicit flow routing and cascading supraglacial lake filling (Banwell et al., 2012; Koziol and Arnold, 2018), the transient filling of supraglacial lakes (Leeson et al., 2012), and flow through predefined channel networks (Yang et al., 2018; Gleason et al., 2021; Yang et al., 2022). In addition to the "damp and delay" behaviour, the supraglacial drainage system evolves on a seasonal timescale. In-situ discharge records from a 0.6 km^2 catchment of the Greenland Ice Sheet reveal changes in the lag time and diurnal amplitude of supraglacial streamflow throughout the 62 day measurement period (Muthyala et al., 2022), suggesting that seasonal changes in the drainage system may also be important in driving changes in subglacial effective pressure.

Here, we investigate the relationship between surface melt and moulin discharge in detail for a small supraglacial catchment on the southwestern Greenland Ice Sheet with a physics-based drainage model. Hill and Dow (2021) first developed the SaDS model and applied it to both a synthetic ice-sheet margin domain and a $\sim 20 \times 27\ \mathrm{km}^2$ catchment of the southwestern Greenland Ice Sheet for the 2013 melt season to validate the model against satellite image-based mapping from late 2013 (Yang and Smith, 2016). We apply the SaDS model to the same catchment for the 2011, 2012, 2015, and 2016 melt seasons to assess how a seasonally-evolving supraglacial drainage system modulates the subglacial drainage system forcing in years with variable melt rates, and how the melt–moulin discharge relationship depends on seasonal melt volume and variability. The model outputs also provide the opportunity to explore the range of supraglacial forcing that may be responsible for triggering supraglacial lake drainage, and to assess interannual patterns in surface drainage in low, average, and high melt years.

2 Data and Methods

2.1 Study Site

We model meltwater flow across a $\sim 20 \times 27\ \mathrm{km}^2$ hydrologic catchment in southwestern Greenland, centered on $67°7'11''\mathrm{N}$, $48°57'37''\mathrm{W}$ (Fig. 1). The site ranges in elevation from approximately 1150 m to 1450 m and falls entirely within the bare ice ablation zone. This region has been the site of previous supraglacial hydrology mapping (Yang and Smith, 2016) and modelling (Hill and Dow, 2021), which have shown that an extensive system of meltwater channels and lakes forms each summer. The four largest lakes in our domain are labelled L1 (elevation 1215 m surface area $1.39 \times 10^6\ \mathrm{m}^2$), L2 (elevation 1218 m, surface area $4.50 \times 10^5\ \mathrm{m}^2$), L3 (elevation 1276 m, surface area $1.04 \times 10^6\ \mathrm{m}^2$), and L4 (elevation 1387 m, surface area $4.86 \times 10^5\ \mathrm{m}^2$). These lakes are small to average size for this portion of western Greenland (e.g. Johansson et al. (2013) report median lake sizes between 1.41 to 2.12 km^2 for west Greenland).

https://doi.org/10.5194/tc-2022-180
Preprint. Discussion started: 27 October 2022
© Author(s) 2022. CC BY 4.0 License.

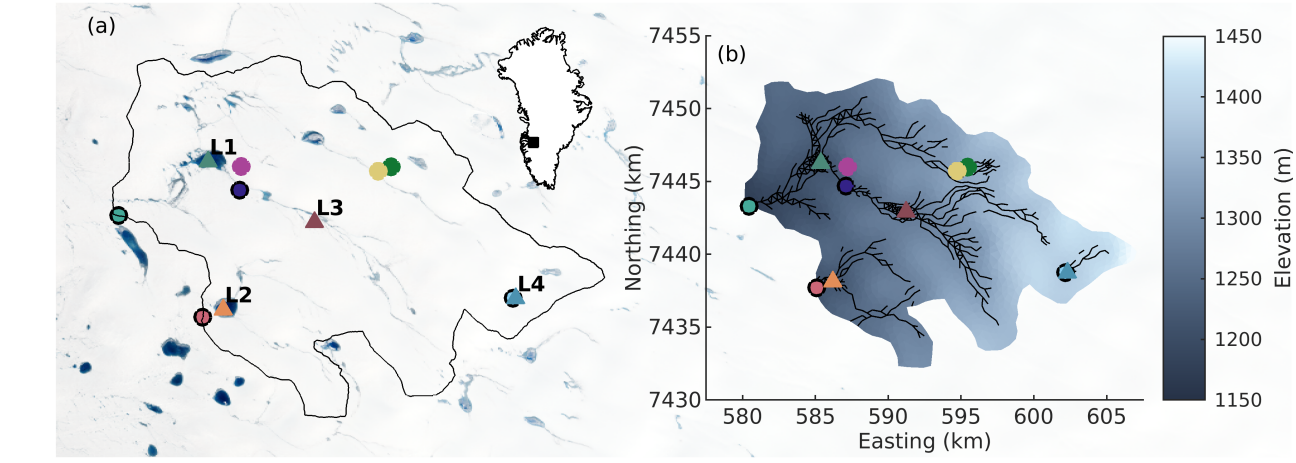

Figure 1. (a) Study domain with moulin locations (circles) previously mapped from a Landsat 8 image (Yang and Smith, 2016) and the four largest supraglacial lakes (triangles). Moulins indicated with a black outline drain one of the four large modelled supraglacial lakes. Background image is a Landsat 8 scene from 8 July 2021. Inset shows location of study site within the Greenland Ice Sheet. (b) Model domain with surface elevation derived from 32 m-resolution ArcticDEM mosaic data (Porter et al., 2018) and modelled supraglacial channel network. Moulins (circles) and lakes (triangles) are as in (a). Coordinates are in UTM 22N projection

2.2 Data

Surface elevations of each element in our triangular computational mesh are computed from ArcticDEM 32 m-resolution mosaic data (Porter et al., 2018). We first smooth the ArcticDEM with a moving average filter with an edge length of 1.44 km, and then average the pixels that lie within each triangular element to define the centroid elevation.

Moulins are placed according to the Landsat-derived map of Yang and Smith (2016), after correcting for off-by-one errors when interpolating onto our triangular mesh and changes in supraglacial water flow paths arising from differences in acquisition time between data used to produce ArcticDEM and the data used to map moulins. Yang and Smith (2016) used a Landsat scene from 19 August 2013 to visually map moulins and supraglacial streams, whereas our DEM represents a combination of data from 2011–2017 (Porter et al., 2018). Since it's possible that supraglacial water flow paths that were present during the acquisition window of ArcticDEM differ from those mapped by Yang and Smith (2016), we have moved moulins by up to 1.29 km (approximately 3× the median edge length in the triangular mesh) to align with flow paths predicted by ArcticDEM.

Surface melt is computed for our domain from RACMO2.3p2 surface melt data at 5.5 km horizontal resolution and 3 hour temporal resolution (Noël et al., 2019). Melt rates from RACMO tiles are linearly interpolated in space and in time to our triangular mesh and to run the model with a timestep of 20 s. We model the years 2011, 2012, 2015, and 2016 so that we can compare moulin inputs for a high melt year (2012) to an average year (2011), and a low melt year (2015) to an average year (2016) (Table S1).

https://doi.org/10.5194/tc-2022-180
Preprint. Discussion started: 27 October 2022
© Author(s) 2022. CC BY 4.0 License.

The Cryosphere Discussions
Open Access
EGU

2.3 Model

We calculate water flow across the surface of the Greenland Ice Sheet and meltwater inputs to moulins using the Subaerial Drainage System (SaDS) model (Hill and Dow, 2021). SaDS is a physics-based model that combines meltwater flow in discrete supraglacial channels and in a distributed water sheet to calculate inputs to moulins. The model explicitly calculates growth and shrinkage of supraglacial meltwater channels in order to capture seasonal changes in moulin inputs. For more details about the model, refer to Hill and Dow (2021). To apply SaDS to our domain, we use an unstructured triangular mesh with 1984 nodes, 3768 elements, 5751 edges, a maximum element area of 1.5×10^5 m^2, and a minimum area of 1.47×10^4 m^2 (Fig. 1).

By applying SaDS to a synthetic ice sheet margin domain, Hill and Dow (2021) found that changes in melt forcing between years led to a shift in the timing of peak moulin inputs. This likely has important implications for subglacial hydrology and ice dynamics, so we explore this hypothesis in more detail here by modelling moulin inputs on the Greenland Ice Sheet in 2011, 2012, 2015, and 2016. We include the potential for persistent supraglacial channels by using the channel configuration from the end of one melt season as initial conditions for the next. The model is spun up using an average melt year (2013) to naturally form an initial supraglacial channel network. The model is then run for the 2011 melt season, and the channels from the end of 2011 are used to initialize the 2012 season. Similarly the model is run for the melt season of 2015 and the outputs from the end of the 2015 run are used to initialize 2016. We expect that incorporating memory of past melt seasons in this way is key to capturing important interannual changes in moulin inputs (Hill and Dow, 2021).

3 Results

By applying SaDS in 2011, 2012, 2015, and 2016, we obtain modelled timeseries of moulin inputs, lake water depth, and water flow across the surface. Moulin inputs broadly track surface melt, with the time-integrated volume dependent on the catchment size, the location of the moulin within the catchment, and, linked to that, the catchment melt volume (Fig. 2). Multi-day increases in melt rate cause a 1–3 day lag in peak moulin input due to the long timescale associated with adjustment in the extent and size of incised supraglacial channels and the damping effects of supraglacial lakes.

In the low or average melt years of 2011, 2015, and 2016, a few intense melt events result in limited short-term (several day) spikes in discharge into moulins (Fig. 2a, b, S1). For example, from 5–21 July 2015, daily peak inputs to the two largest moulins are consistently above 30 m^3 s^{-1}, except for a period of reduced melt from 12–15 July, compared to an average of < 24 m^3 s^{-1}. In the high melt year of 2012, frequently recurring intense melt events result in persistently high discharge into moulins with large differences between minimum discharge, occurring between melt events, and peak discharge, occurring during melt events (Fig. 2a). For example, moulin inputs reach a local minimum of 8.6 m^3 s^{-1} at 08:00 local time on 23 July 2012, and a maximum of 51.1 m^3 s^{-1} five days later at 14:00 on 28 July 2012. The maximum discharge of 70.3 m^3 s^{-1} at 20:00 11 July 2012, driven by domain-averaged melt rates of 7.3 cm day^{-1} on 10 July, was preceded by a discharge of just 31.6 m^3 s^{-1} at 06:00 8 July. These differences in melt are much greater than the typical diurnal variability of < 10 m^3 s^{-1}.

Compared to surface melt, which has a diurnal amplitude of nearly 100% (i.e., melt pauses overnight), the amplitude of moulin inputs is strongly damped. For moulins that do not drain one of the four largest supraglacial lakes (i.e., for moulins with

https://doi.org/10.5194/tc-2022-180
Preprint. Discussion started: 27 October 2022
© Author(s) 2022. CC BY 4.0 License.

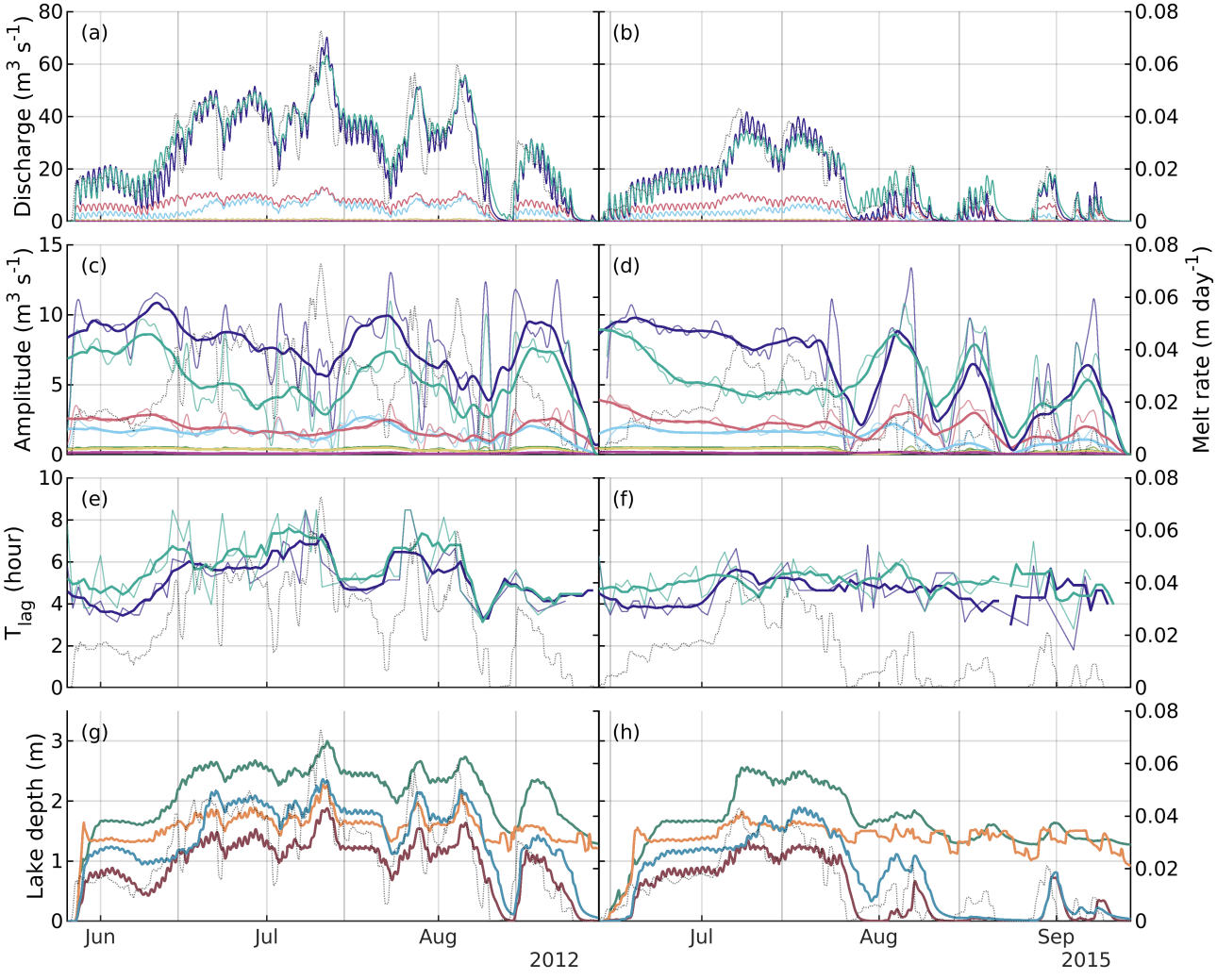

Figure 2. (a, b) Moulin hydrographs (colours, corresponding to moulin markers in Fig. 1) and 24-hour moving average RACMO2.3p2 ice surface melt rates (black). Right axis (dotted line) shows 24-hour rolling average melt rate. (c, d) Diurnal amplitude of discharge into moulins in 2012 and 2015. Light colours show instantaneous diurnal amplitude, and bold colours show the seven-day moving average diurnal amplitude. (e, f) Lag time between local solar noon (∼15:22) and peak moulin discharge for the two moulins with the highest discharge rates. (g, h) Supraglacial lake water depths for lakes L1 (green, elevation 1215 m), L2 (gold, elevation 1218 m), L3 (red, elevation 1276 m), and L4 (blue, elevation 1387 m).

https://doi.org/10.5194/tc-2022-180
Preprint. Discussion started: 27 October 2022
© Author(s) 2022. CC BY 4.0 License.


no black outline in 1), diurnal amplitude is typically 25–50% of the mean discharge. The four large supraglacial lakes further damp the diurnal melt signal of downstream moulins, which have a diurnal amplitude of only 10–25% of the mean discharge (Fig. 2c, d, S2).

The seven-day moving average diurnal amplitude reveals some interesting short-term trends in the first few weeks of the melt season. In 2011 and 2015, the diurnal amplitude of moulin inputs distinctly decreases throughout the first few weeks of the melt season (Fig. 2d, S2). In 2012, this decreasing trend begins later, once melt rates begin to stabilize in late June (Fig. 2c).

Several supraglacial lakes fill and overflow within the domain. The four largest lakes, shown in Fig. 1, fill quickly in the first few weeks of the melt season (Fig. 2g, h, S4). Lake L1 fills and drains more slowly than the other lakes due to its larger surface area (34% larger surface area than the second largest lake, L3). The highest elevation lake, L4 (elevation 1387 m), fills noticeably later (4 days later in 2015) than the other lakes (elevations 1215–1276 m), except in 2012 where melt occurred throughout the entire domain at the initial onset of positive air temperatures.

The supraglacial channel network itself evolves on an annual basis. Over the course of the melt season, the cumulative length of incised supraglacial channels decreases by up to 30% by peak melt, before increasing again back to approximately the original length (Fig. S5). Most of this change is due to the melt out of small channels (defined as those with incision depth $H_c \leq 0.3$ m). The cumulative length of large channels ($H_c > 0.3$ m) seasonally changes by up to 20% under intense melt conditions in 2012, but only $\sim 10\%$ under low melt conditions in 2015. Large channels are therefore more likely to be perennial features compared to small channels, yet large channels still undergo significant seasonal changes in their extent.

4 Discussion

4.1 Seasonal trends in drainage system behaviour

The early-season decrease in moulin diurnal amplitude observed in 2011 and 2015 (Fig. 2d, S2) is likely attributable to changes in the extent of the supraglacial channel network. As small channels melt out, meltwater must first flow through the slow, distributed system before it intersects a large, perennial channel. Since hillslope flow occurs slowly compared to channelized flow, the melt-out of small channels increases the difference in transport time between locations close to and far from perennial channels, reducing the diurnal amplitude of moulin inputs.

In-situ streamflow observations from a 0.6 km^2 catchment in southwestern Greenland show a statistically significant decrease in the lag time between local solar noon and peak moulin inputs in the first few weeks of the melt season (Muthyala et al., 2022). Our simulations, however, do not support a consistent trend (Fig. 2e, f). In the high melt year 2012, lag time ranges from ~4 to 8 hours, and in 2015 lag time is between 4 and 6 hours. The lack of a consistent trend may, in part, be explained by the larger size of our domain and the number of supraglacial lakes compared to the small, lake-free domain of Muthyala et al. (2022).

https://doi.org/10.5194/tc-2022-180
Preprint. Discussion started: 27 October 2022
© Author(s) 2022. CC BY 4.0 License.


4.2 Influence of supraglacial lakes

The lag time between local solar noon and peak moulin inputs does not appear to be directly related to the rate of surface melt in our model, but instead is correlated to lake water level ($r = 0.62$ between water depth in lake L1 and lag time for the largest moulin). This correlation suggests that perhaps lag time is related to the amount of water stored in the domain, since larger lakes should further delay the melt response. It is important to note here that our melt forcing data have a temporal resolution of 3 hours (Noël et al., 2019), so it remains difficult to smoothly constrain the time of minimum moulin inputs at sub-hourly resolution. This pattern can not be compared to the observations of Muthyala et al. (2022) as their domain does not include a supraglacial lake.

Our modelled supraglacial lakes also respond dynamically to changes in surface melt intensity (Fig. 2g, h). The lake water depth quickly rises within the first few weeks of the melt season. Once the melt rate peaks, the lakes fill beyond their original outlet elevation as water floods regions of low surface slope along the outlet path. Lake L1 fills to more than 1 m above its original outlet elevation since it drains a large area and it lies in a broad topographic low with very low slope (Fig. 1). Since each lake drains through a different moulin, there is no evidence of cascading lake drainage in our particular model domain.

The fact that lake water level does not simply saturate at the outlet elevation has implications for rapid lake drainage. If rapid hydrofracture drainage events are at least partially controlled by water level (and therefore pressure), the fast water level fluctuations we have predicted may partly explain why it has been difficult to constrain the drainage trigger mechanism (e.g. Banwell et al., 2012; Poinar and Andrews, 2021).

4.3 Interactions between drainage system components

The pattern of temporally varying lake water level is a result of interactions between the distributed and channelized systems (Fig. 3a). For low meltwater supply, when the channel network has not reached its maximum capacity, channels efficiently route flow from the distributed system towards supraglacial lakes and moulins. Increases in melt production are accommodated through greater flow through both modes of drainage, as evidenced by the positive correlation between the total volume of water in the channel and sheet systems in the bottom left quadrant of Fig. 3a. As melt rates increase, water flow in the channel network reaches its capacity. For our catchment, this occurs for a total mass in the channels of $\sim 4 \times 10^8$ kg. As channels become fully saturated, water is forced to flood the distributed system, overfilling supraglacial lakes as their outlet channels are overwhelmed. The point at which channels become saturated is shown by the turning point in Fig. 3a. In this regime, a small increase in the volume of water flowing through the channel system is associated with large increase in the volume of water flowing through the distributed system and the stored in supraglacial lakes, resulting in highly dynamic lake water levels.

We can assess how lake filling and draining directly control moulin inputs by comparing water level in lake L1 with discharge through the moulin that drains lake L1's catchment (Fig. 3b). In the early melt season when L1 is filling, the lake water depth and moulin discharge are uncorrelated since the lake is not yet overflowing and contributing to discharge into the moulin. When the lake begins to overflow and drain through its outlet, which for L1 occurs above 1.5 m water depth, the moulin discharge and lake depth become correlated. At this point, water draining from the lake is a major contributor to flow into the moulin, as

https://doi.org/10.5194/tc-2022-180
Preprint. Discussion started: 27 October 2022
© Author(s) 2022. CC BY 4.0 License.

The Cryosphere Discussions
Open Access
EGU

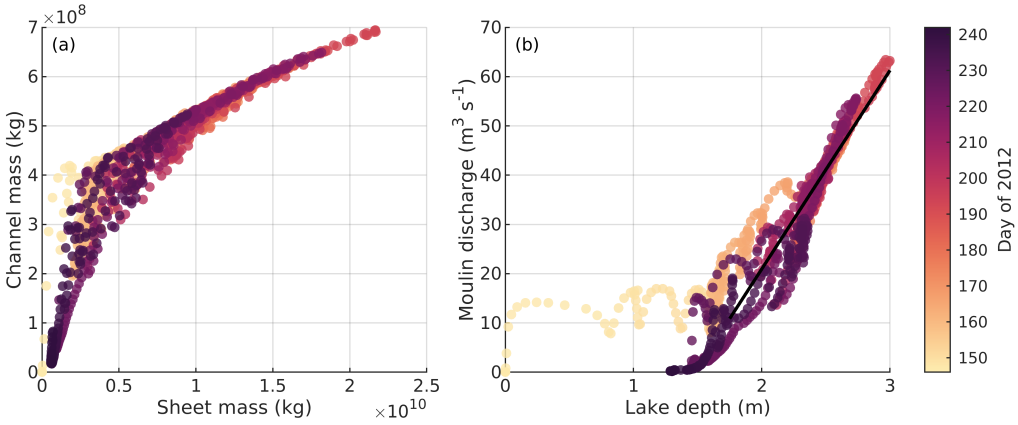

Figure 3. (a) Relationship between total water mass flowing through supraglacial channels and within the distributed water sheet for the 2012 melt season. (b) Relationship between moulin discharge and lake depth for 2012 for lake L1 (green in Fig. 1; elevation 1215 m) and its outlet moulin (red in Fig. 1, coordinates (580.4 km N, 7443 km E)). The black line is a linear fit through the data points with lake depth ≥ 1.75 m ($r^2 = 0.84$).

evidenced by the close fit to the black line in Fig. 3b (correlation $r^2 = 0.84$). Meltwater from the rest of the catchment that does not flow through L1 still contributes to the moulin discharge since lake depth does not describe all of the variation in moulin discharge (correlation < 1). Under intense surface melt, when water depth in the lake increases above 2.5 m, lake water depth and moulin discharge are almost exactly linearly related, with correlation $r^2 = 0.93$. For low moulin discharge and lake water depth, which occurs when surface melt pauses and at the end of the melt season, lake depth and moulin discharge taper off simultaneously. This suggests that slow lake drainage at the end of the melt season is responsible for the gradual shut down of moulin inputs after melt ceases in Fig. 2. These relationships are collectively modulated by the finite time it takes water that spills out of the lake to reach the moulin. This time delay is responsible for the hysteresis-like loops in Fig. 3b. Once the lake is full, changes in lake depth occur before the associated response in moulin discharge, hence the counter-clockwise loops for lake depth >1.5 m.

4.4 Model intercomparison

These model outputs provide an interesting context to compare the SaDS model to existing supraglacial drainage models. The Surface Routing and Lake Filling model (SRLF; Banwell et al., 2012; Koziol and Arnold, 2018) is a single-component model intended to represent the filling and draining of supraglacial lakes. SRLF explicitly evacuates all excess water from lakes to the downstream drainage pathway, so that lake level saturates at exactly the outlet elevation. This saturation would result in a flat water level in Fig. 2g, h. SaDS permits excess water to be transiently stored in lakes according to the distributed sheet flow model, leading to a dynamic lake water level (Fig. 2g, h) and a slow, extended taper off of moulin inputs at the end of the melt season as the lakes slowly overspill (Figs. 2, 3).

https://doi.org/10.5194/tc-2022-180
Preprint. Discussion started: 27 October 2022
© Author(s) 2022. CC BY 4.0 License.


The supraglacial lake model by Leeson et al. (2012) is similar to the lake formulation of SaDS. Both Leeson et al. (2012) and SaDs compute the flow direction based on combined ice and water sheet surface elevation, compared to SRLF which is based on the ice surface elevation alone. Using the free surface elevation to determine flow direction and velocity allows lakes to form naturally as regions with flat surfaces that are located in hydraulic minimums, instead of requiring lakes to form in pre-specified basins. It also removes the condition that the DEM must have its sinks filled since these will naturally accumulate water. Rather than being first specified as a continuous partial differential equation model before being discretized, Leeson et al. (2012) present the fully numerically discretized model based on physical arguments about water flow between neighbouring cells. The resulting model is similar to the distributed 'sheet' flow model of SaDS, although Leeson et al. (2012) do not consider additional melt due to heat dissipation within the flowing water layer.

Compared to Leeson et al. (2012) and the SRLF model, SaDS includes discrete drainage channels incised into the ice surface. In the context of lake filling, discrete channels are important for allowing lakes to fill quickly in the early melt season by efficiently routing large volumes of runoff into the lake basin. Including both components is especially important for catchments spanning a wide elevation range, since the drainage density, and therefore the drainage system capacity, is sensitive to elevation-dependent melt rates (Yang et al., 2022). Both components have been included in the Rescaled Width Function (RWF) model produced by Yang et al. (2018). The RWF model, however, does not model the filling and draining of supraglacial lakes. It also requires an arbitrary specification of the time evolution of the drainage density. SaDS instead computes the channel network according to approximate channel evolution physics. The physics-based, transient formulation of SaDS makes it significantly more computationally expensive than other models (∼7 days per year of simulation time in the configuration presented here), so it is most applicable when the subtle details of the supraglacial drainage system are important.

5 Conclusions

We have presented model outputs of supraglacial meltwater flow, lake filling and draining, and surface inputs to moulins for a small catchment on the Greenland Ice Sheet for four years, including the extreme melt year in 2012. These outputs point to the dynamic nature of the supraglacial drainage system.

To first order, moulin inputs, modelled with the Subaerial Drainage System (SaDS) model, follow surface melt. Diurnal cycles in melt are strongly damped, while multi-day melt pulses are not, both of which are likely transmitted to the subglacial drainage system. Moreover, the response to surface melt is dynamic through the melt season as the supraglacial channel network contracts and expands. In years with steady melt rates in the early melt season, the diurnal amplitude decreases as the drainage system evolves. In the high melt year of 2012, seasonal patterns are instead dominated by frequent and recurring periods of intense surface melt. The seasonal decreasing trend in moulin diurnal amplitude that is visible in the low melt year 2015 is not clear in 2012, suggesting that high and variable surface melt rates disrupt the otherwise predictable seasonal evolution of the supraglacial drainage system.

The highly dynamic supraglacial hydrology that we have described here demands that surface flow should not be neglected in modelling the connection between surface melt and ice dynamics. Since the subglacial drainage system is sensitive to the

https://doi.org/10.5194/tc-2022-180
Preprint. Discussion started: 27 October 2022
© Author(s) 2022. CC BY 4.0 License.


volume and duration of meltwater inputs (Bartholomew et al., 2012; Hewitt, 2013), it is important to use realistic moulin inputs to drive subglacial models, such as those presented here with the Subaerial Drainage System (SaDS) model.

Code and data availability. ArcticDEM data are freely available from the Polar Geospatial Center (https://www.pgc.umn.edu/data/arcticdem/). RACMO surface melt data are available by contacting the Institute for Marine and Atmospheric research Utrecht University (https://www.projects.science.uu.nl/iceclimate/models/racmo.php). The SaDS model is described fully in Hill and Dow (2021) including equations and implementation. Parameters for model application are supplied in Table S2. Model outputs and code to produce the figures are available at https://doi.org/10.5281/zenodo.6094396.

Author contributions. T Hill contributed to conceptualization, analysis, methodology, software, visualization, writing and reviewing. C Dow contributed to conceptualization, analysis, methodology, supervision, and reviewing & editing.

Competing interests. The authors declare that they have no conflict of interest.

Acknowledgements. T Hill was supported by the Ontario Graduate Scholarship and NSERC Canada Graduate Scholarship programs. C Dow was supported by the Natural Sciences and Engineering Research Council of Canada (RGPIN-03761-2017) and the Canada Research Chairs Program (950-231237). The authors declare that they have no conflicts of interest. DEM provided by the Polar Geospatial Center under NSF-OPP awards 1043681, 1559691, and 1542736. The authors would like to thank Brice Noël and Michiel van den Broeke for providing RACMO surface melt data.

https://doi.org/10.5194/tc-2022-180
Preprint. Discussion started: 27 October 2022
© Author(s) 2022. CC BY 4.0 License.


References

Banwell, A. F., Arnold, N. S., Willis, I. C., Tedesco, M., and Ahlstrøm, A. P.: Modeling supraglacial water routing and lake filling on the Greenland Ice Sheet, Journal of Geophysical Research: Earth Surface, 117, https://doi.org/10.1029/2012JF002393, 2012.

Bartholomew, I., Nienow, P., Sole, A., Mair, D., Cowton, T., and King, M. A.: Short-term variability in Greenland Ice Sheet motion forced by time-varying meltwater drainage: Implications for the relationship between subglacial drainage system behavior and ice velocity, Journal of Geophysical Research: Earth Surface, 117, https://doi.org/10.1029/2011JF002220, 2012.

Gleason, C. J., Yang, K., Feng, D., Smith, L. C., Liu, K., Pitcher, L. H., Chu, V. W., Cooper, M. G., Overstreet, B. T., Rennermalm, A. K., et al.: Hourly surface meltwater routing for a Greenlandic supraglacial catchment across hillslopes and through a dense topological channel network, The Cryosphere, 15, 2315–2331, https://doi.org/10.5194/tc-15-2315-2021, 2021.

Goelzer, H., Nowicki, S., Payne, A., Larour, E., Seroussi, H., Lipscomb, W. H., Gregory, J., Abe-Ouchi, A., Shepherd, A., Simon, E., et al.: The future sea-level contribution of the Greenland ice sheet: a multi-model ensemble study of ISMIP6, The Cryosphere, 14, 3071–3096, https://doi.org/10.5194/tc-14-3071-2020, 2020.

Hewitt, I.: Seasonal changes in ice sheet motion due to melt water lubrication, Earth and Planetary Science Letters, 371, 16–25, https://doi.org/10.1016/j.epsl.2013.04.022, 2013.

Hill, T. and Dow, C. F.: Modeling the Dynamics of Supraglacial Rivers and Distributed Meltwater Flow With the Subaerial Drainage System (SaDS) Model, Journal of Geophysical Research: Earth Surface, 126, e2021JF006 309, https://doi.org/https://doi.org/10.1029/2021JF006309, 2021.

Johansson, A., Jansson, P., and Brown, I.: Spatial and temporal variations in lakes on the Greenland Ice Sheet, Journal of Hydrology, 476, 314–320, https://doi.org/https://doi.org/10.1016/j.jhydrol.2012.10.045, 2013.

Koziol, C. P. and Arnold, N.: Modelling seasonal meltwater forcing of the velocity of land-terminating margins of the Greenland Ice Sheet, The Cryosphere, 12, 971–991, https://doi.org/10.5194/tc-12-971-2018, 2018.

Leeson, A. A., Shepherd, A., Palmer, S., Sundal, A., and Fettweis, X.: Simulating the growth of supraglacial lakes at the western margin of the Greenland ice sheet, The Cryosphere, 6, 1077–1086, https://doi.org/10.5194/tc-6-1077-2012, 2012.

Moon, T., Joughin, I., Smith, B., and Howat, I.: 21st-century evolution of Greenland outlet glacier velocities, Science, 336, 576–578, https://doi.org/10.1126/science.1219985, 2012.

Mouginot, J., Rignot, E., Bjørk, A. A., Van den Broeke, M., Millan, R., Morlighem, M., Noël, B., Scheuchl, B., and Wood, M.: Forty-six years of Greenland Ice Sheet mass balance from 1972 to 2018, Proceedings of the national academy of sciences, 116, 9239–9244, https://doi.org/10.1073/pnas.1904242116, 2019.

Muthyala, R., Rennermalm, Å. K., Leidman, S. Z., Cooper, M. G., Cooley, S. W., Smith, L. C., and van As, D.: Supraglacial streamflow and meteorological drivers from southwest Greenland, The Cryosphere, 16, 2245–2263, https://doi.org/10.5194/tc-16-2245-2022, 2022.

Noël, B., van de Berg, W. J., Lhermitte, S., and van den Broeke, M. R.: Rapid ablation zone expansion amplifies north Greenland mass loss, Science Advances, 5, https://doi.org/10.1126/sciadv.aaw0123, 2019.

Poinar, K. and Andrews, L. C.: Challenges in predicting Greenland supraglacial lake drainages at the regional scale, The Cryosphere, 15, 1455–1483, https://doi.org/10.5194/tc-15-1455-2021, 2021.

Porter, C., Morin, P., Howat, I., Noh, M.-J., Bates, B., Peterman, K., Keesey, S., Schlenk, M., Gardiner, J., Tomko, K., Willis, M., Kelleher, C., Cloutier, M., Husby, E., Foga, S., Nakamura, H., Platson, M., Wethington, Michael, J., Williamson, C., Bauer, G.,

https://doi.org/10.5194/tc-2022-180
Preprint. Discussion started: 27 October 2022
© Author(s) 2022. CC BY 4.0 License.

Enos, J., Arnold, G., Kramer, W., Becker, P., Doshi, A., D'Souza, C., Cummens, P., Laurier, F., and Bojesen, M.: ArcticDEM, https://doi.org/10.7910/DVN/OHHUKH, 2018.

Schoof, C.: Ice-sheet acceleration driven by melt supply variability, Nature, 468, 803–806, https://doi.org/10.1038/nature09618, 2010.

Sole, A., Nienow, P., Bartholomew, I., Mair, D., Cowton, T., Tedstone, A., and King, M. A.: Winter motion mediates dynamic response of the Greenland Ice Sheet to warmer summers, Geophysical Research Letters, 40, 3940–3944, https://doi.org/10.1002/grl.50764, 2013.

Sundal, A. V., Shepherd, A., Nienow, P., Hanna, E., Palmer, S., and Huybrechts, P.: Melt-induced speed-up of Greenland ice sheet offset by efficient subglacial drainage, Nature, 469, 521–524, https://doi.org/10.1038/nature09740, 2011.

The IMBIE Team: Mass balance of the Greenland Ice Sheet from 1992 to 2018, Nature, 579, 233–239, https://doi.org/10.1038/s41586-019-1855-2, 2020.

van den Broeke, M., Box, J., Fettweis, X., Hanna, E., Noël, B., Tedesco, M., van As, D., van de Berg, W. J., and van Kampenhout, L.: Greenland ice sheet surface mass loss: recent developments in observation and modeling, Current Climate Change Reports, 3, 345–356, https://doi.org/10.1007/s40641-017-0084-8, 2017.

Yang, K. and Smith, L. C.: Internally drained catchments dominate supraglacial hydrology of the southwest Greenland Ice Sheet, Journal of Geophysical Research: Earth Surface, 121, 1891–1910, https://doi.org/10.1002/2016JF003927, 2016.

Yang, K., Smith, L. C., Karlstrom, L., Cooper, M. G., Tedesco, M., van As, D., Cheng, X., Chen, Z., and Li, M.: A new surface meltwater routing model for use on the Greenland Ice Sheet surface, The Cryosphere, 12, 3791–3811, https://doi.org/10.5194/tc-12-3791-2018, 2018.

Yang, K., Smith, L. C., Andrews, L. C., Fettweis, X., and Li, M.: Supraglacial Drainage Efficiency of the Greenland Ice Sheet Estimated From Remote Sensing and Climate Models, Journal of Geophysical Research: Earth Surface, 127, e2021JF006 269, https://doi.org/https://doi.org/10.1029/2021JF006269, 2022.

Zwally, H. J., Abdalati, W., Herring, T., Larson, K., Saba, J., and Steffen, K.: Surface melt-induced acceleration of Greenland ice-sheet flow, Science, 297, 218–222, https://doi.org/10.1126/science.1072708, 2002.